

Stress-field evolution during the 26 November 2019 Durrës (Albania) earthquake sequence: co-seismic, early post-seismic, and tectonic-region inversions

¹Edmond Dushi, Besian Rama, Damiano Koxhaj

Institute of Geosciences (IGEO), Polytechnic University of Tirana, Tirana, Albania

Abstract

We resolve the stress field associated with the 26 November 2019 Mw 6.3 Durrës earthquake sequence through three windows: the co-seismic mainshock, the early post-seismic phase (mainshock plus the 36 largest aftershocks recorded between 26 November and 2 December 2019), and a regional tectonic subset of 27 moderate-magnitude events. The co-seismic stress tensor is obtained by inverting the moment-tensor solutions reported by the contributing agencies for the mainshock. In contrast, the regional and immediate post-seismic stress fields are derived from previously published focal-mechanism and moment-tensor solutions, both from the existing report and from the continuously updated archive of mechanisms for the sequence, using the StressInverse methodology and assuming both nodal planes where required. Regional inversions define a persistent WSW–ENE compressional regime with a shallowly plunging σ_1 axis and a steeply plunging σ_3 axis. The early sequence preserves this compression orientation but shifts to lower φ and μ values ($\varphi \approx 0.546$; $\mu \approx 0.45$), indicating transient coseismic relaxation and short-lived stress redistribution following the mainshock. These changes imply a temporary reduction in deviatoric stress and a more oblate post-seismic configuration without rotation of the principal-stress axes. The TENSOR solution confirms reverse-faulting kinematics for the mainshock, and the recovered σ_1 azimuth (≈ 239 – 248°) is consistent with present-day Adria–Eurasia convergence and the mapped thrust architecture of the Outer Albanides. Transient changes in φ and μ are consistent with short-lived coseismic relaxation and apparent weakening during rupture.

Keywords: Stress inversion; Focal mechanisms; Coseismic relaxation; Deviatoric stress; Durrës earthquake sequence.

1 Study area and datasets

The Durrës–Tirana area lies in the western Albanian Periadriatic foreland, along the contact where the Adria microplate underthrusts the Eurasian margin within the Albanides collision zone [1, 2, 3]. In this region, reverse and oblique-reverse faulting is supported by the spatially coherent pattern of focal mechanism and moment tensor solutions (Figs. 1–2). When viewed together with detailed geological mapping [3, 4, 5] and published GPS-velocity fields [6,7,

¹ Corresponding author: e.dushi@geo.edu.al

8, 9], these mechanisms delineate an active WSW–WSW-WSW-ENE-oriented shortening belt characteristic of the outer Albanides [4–10]. This pattern agrees with regional deformation studies across the Adriatic–Aegean system and with the established seismotectonic framework of Albania [11–13], and is consistent with independent focal-mechanism compilations for Albania and neighboring regions [14–17].

The inputs used in this study consist exclusively of published focal-mechanism (FM) and moment-tensor (MT) solutions provided by major monitoring and research institutions, including the Institute of Geosciences, Polytechnic University of Tirana (IGEO); the National Observatory of Athens (NOA); the Aristotle University of Thessaloniki (AUTH); the National Institute of Geophysics and Volcanology (INGV); the United States Geological Survey (USGS); the German Research Centre for Geosciences (GFZ); and the Global Centroid Moment Tensor project (GCMT). For the mainshock and the very-early aftershock activity, MT information is taken from NOA solutions documented in the EMSC early-sequence report [18].

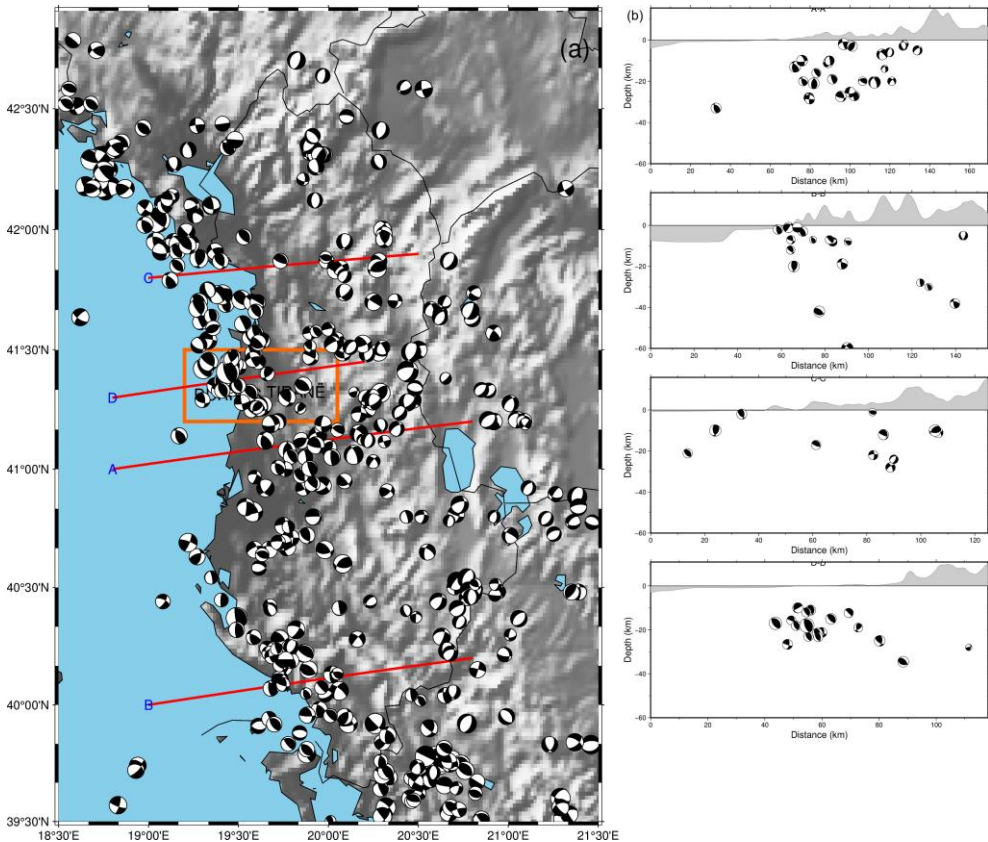


Fig. 1. (a)- Regional focal-mechanism map; (b) - cross sections D–D', A–A', B–B', and C–C' of focal mechanisms; Durrës–Tirana study area (orange rectangle), (generated with PyGMT [19] and GMT 6 [20]).

Additional regional MT solutions were obtained from the published catalogues of the agencies mentioned earlier. Time-domain MT solutions were taken from the NOA and AUTH catalogue products, which rely on the ISOLA and GISOLA inversion workflows [21]. Regional focal-mechanism information for Albania and the surrounding areas was obtained from published catalogues [14–17] and complemented by Albania-specific studies [22–23]. All FM and MT solutions were used exactly as published.

Two datasets were prepared for the stress inversion analysis. The regional dataset consists of 27 FM/MT solutions from the wider Durrës–Tirana area; for these events, two nodal-plane selection schemes (dr_planA and dr_planB) were applied to evaluate the impact of plane choice on inversion stability. The sequence dataset includes the mainshock and the 36 largest aftershocks recorded between 26 November and 2 December 2019, representing the very-early post-seismic adjustment stage and enabling direct comparison with the long-term regional reference. The sequence composition follows the event set documented in the EMSC report [18].

Figure 1 illustrates the tectonic setting and spatial distribution of regional FM and MT solutions together with four longitudinal cross-sections (D–D', A–A', B–B', C–C') that depict depth variability of the focal mechanism along the coastal belt. Figure 2 focuses on the Durrës epicentral area and shows the focal mechanisms used for the co-seismic and early post-seismic stress comparisons [11–14, 18].

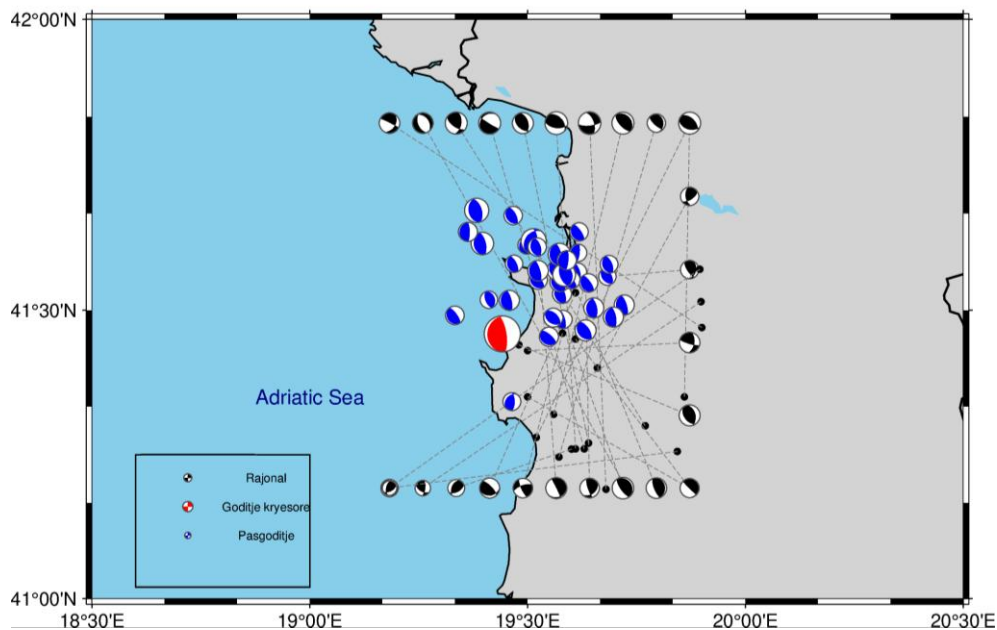


Fig. 2. Durrës area moment tensors: **mainshock** (red), **aftershocks** (blue; 26 Nov–2 Dec 2019), and **regional** mechanisms (black/grey); symbol size \propto Mw (generated with PyGMT [19] and GMT 6 [20]).

2 Method

Co-seismic (mainshock) stress was estimated using the TENSOR methodology based on the Right-Dihedron approach and rotational optimization [24]. The Right-Dihedron method partitions the focal sphere into compressional and tensional dihedra and, for each trial stress tensor, selects the nodal plane that best matches the observed first-motion polarities and rake. This procedure reduces the ambiguity associated with the two possible fault planes of each focal mechanism. The inversion searches for the orientation of the principal stresses and the reduced-stress ratio ϕ by minimizing the summed slip-angle misfit for all events. The slip-angle misfit is defined as:

$$\psi_i = \text{Arcos} (d_i \cdot \tau_i / |\tau_i|) \quad (1)$$

where d_i is the unit slip (rake) vector from the observed focal mechanism of event i , τ_i is the shear traction acting on the selected fault plane, and ψ_i is the angular difference between the observed and model-predicted slip direction.

Trial stress tensors are expressed using a principal-stress parameterization, in which the Cauchy stress tensor σ is written as:

$$\sigma = R \cdot \text{diag} (\sigma_1, \sigma_2, \sigma_3) \cdot R^T \quad (2)$$

where R is a rotation matrix defining the orientation of the principal stresses, and $\sigma_1 \geq \sigma_2 \geq \sigma_3$ denote the maximum, intermediate, and minimum compressive stresses. The reduced-stress ratio ϕ describes the relative position of σ_2 between σ_1 and σ_3 and is defined as:

$$\phi = (\sigma_2 - \sigma_3) / (\sigma_1 - \sigma_3) \quad (3)$$

For any candidate fault plane with unit normal vector n , the stress acting on the plane is obtained from standard Cauchy relations. The traction vector acting on the plane is $t = \sigma \cdot n$; the normal stress is $\sigma_n = n \cdot t$; and the shear traction is the component tangential to the plane, $\tau = t - \sigma_n n$. These relations follow the Wallace–Bott formulation [25, 26], which assumes that slip occurs in the direction of maximum shear traction. This provides the physical connection between the stress tensor and the observed focal mechanisms.

Early post-seismic (mainshock + 36 events, 26 November–2 December 2019) and regional (27 mechanisms; `dr_planA/dr_planB`) stress states were determined using the `pyStress/StressInverse` algorithm following the formulations of Michael [27–30]. For each trial stress tensor, both nodal planes of every focal mechanism are evaluated, and the plane producing the smaller misfit ψ_i (Eq. 1) is selected. The inversion jointly solves for the orientations of $\sigma_1, \sigma_2, \sigma_3$, and the reduced-stress ratio ϕ (Eq. 3), ensuring internal compatibility between the predicted shear tractions and the observed slip vectors.

To compare the tendency of faults to slip across the coseismic, early post-seismic, and regional windows, a slip-tendency parameter was computed:

$$F = |\tau| - \mu \sigma'_n \quad (4)$$

where $|\tau|$ is the magnitude of the shear traction, σ'_n is the effective normal stress, and μ is an effective friction coefficient used here as a proxy parameter rather than a quantity fitted during inversion. In this study, μ captures the relative resistance to slip and is used to track changes in fault stability between windows. The value inferred for the early post-seismic window ($\mu \approx 0.45$) indicates a temporary coseismic reduction in effective friction, consistent with transient weakening mechanisms, short-lived stress redistribution, and a more oblate

post-seismic stress configuration without rotation of the principal-stress axes. Lower μ values, therefore, reflect relaxation and reduced deviatoric stress immediately following the mainshock.

All focal-mechanism (FM) and moment-tensor (MT) inputs used in the inversions correspond exactly to the published solutions obtained from the contributing institutions and catalogues described in the data section. Time-domain MT solutions from NOA and AUTH [15-18], computed using the ISOLA and GISOLA workflows [21], were incorporated directly as published. No waveform re-inversions were performed.

Table 1. Data windows and sources used in the inversions.

Window	Time span	N events	Primary sources	Inversion
Co-seismic	26 Nov 2019 (mainshock)	1	NOA/IGEO, INGV, USGS, GFZ, GCMT, AUTH	TENSOR
Early post-seismic	26 Nov–2 Dec 2019	37 (incl. mainshock)	NOA/IGEO sequence MTs	StressInverse
Tectonic-region	1964–present (subset)	27	Regional catalogs (e.g., Ormeni et al., 2022)	StressInverse

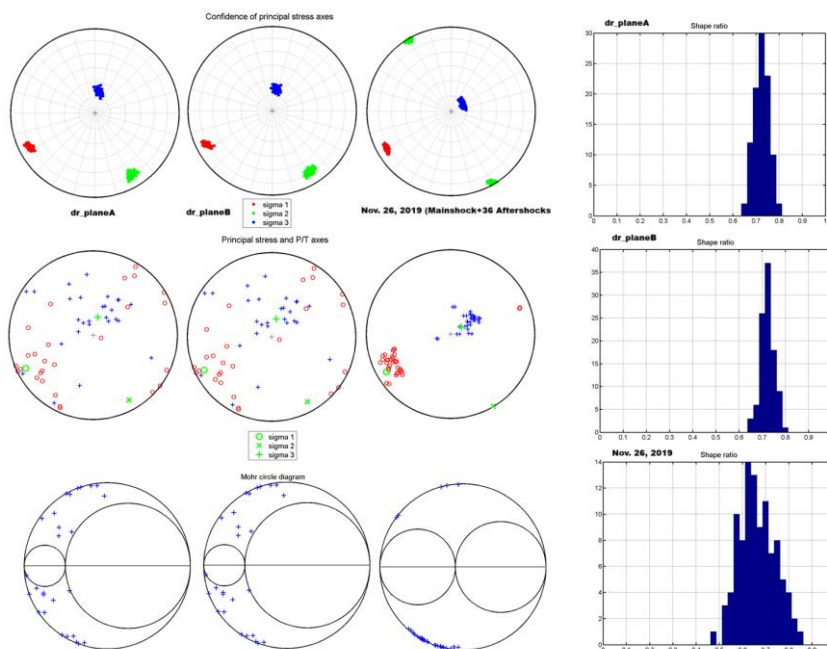


Fig. 3. StressInverse outputs for tectonic-region (dr_planA, dr_planB) and early post-seismic sequence: σ -axis clusters, P/T stereograms, Mohr diagrams, ϕ histograms.

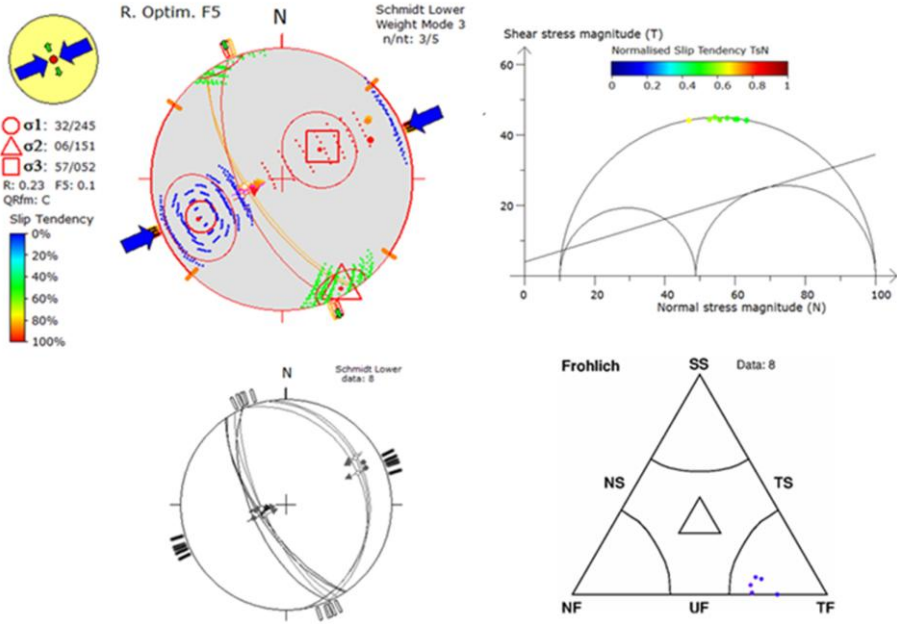


Fig. 4. TENSOR mainshock solution using Right Dihedron and rotational optimization (co-seismic stress tensor and associated dihedron panel).

3 Results and discussion

Regional inversions converge on a WSW–ENE–directed compressional regime characterized by shallow-plunging σ_1 (dr_planA: 246.9/8.1°, dr_planB: 248.0/6.9°) and steep σ_3 (dr_planA: 14.0/76.7°, dr_planB: 16.8/77.4°). These solutions are associated with elevated φ and μ values (0.75/0.70; 0.95/0.93), consistent with an active reverse-faulting stress field. The early post-seismic inversion yields $\sigma_1 = 239.5/12.5^\circ$, $\sigma_2 = 149.3/0.5^\circ$, $\sigma_3 = 57.2/77.5^\circ$, together with $\varphi = 0.546$ and $\mu = 0.45$. The co-seismic analysis confirms a pure reverse-faulting regime broadly aligned with the regional shortening field. The persistence of the σ_1 azimuth and its shallow plunge across all windows agrees with the long-term deformation patterns mapped in the broader Adriatic–Aegean system [1-5], and is consistent with stress-field signatures reported in the post-event geodetic and seismotectonic analyses of the Durrës earthquake [31].

The azimuthal stability of σ_1 across regional, co-seismic, and early post-seismic windows also matches the GPS-inferred convergence direction between Adria and Eurasia [6-9], and is compatible with the mapped thrust geometries of the Outer Albanides [10-14]. These consistencies indicate that the 2019 sequence was governed by the same compressional stress field active at the scale of the western Balkan foreland.

A key feature of the early post-seismic solution is the significant reduction in φ and μ relative to the regional and co-seismic states. The decrease in μ (≈ 0.45) reflects a temporary decrease in shear resistance and a more oblate stress ellipsoid, suggestive of transient fault-zone weakening shortly after the mainshock. This pattern is consistent with friction-reducing

processes and co-seismic stress relaxation predicted by constitutive friction models [33], as well as with the short-term adjustments observed in structural and kinematic studies of the 2019 Durrës seismogenic system.

Our findings also align with stress-inversion studies based on focal mechanisms for the same sequence. Teloni et al. (2021) [34] documented a reverse-faulting stress regime with $\sigma_1 \approx 241^\circ/15^\circ$ and $\sigma_3 \approx 025^\circ/72^\circ$, using Win-Tensor and rotational optimization, obtaining a stress-ratio estimate of $R = 0.5$ and a World Stress Map (WSM) quality ranking of B as classified in Heidbach et al. (2016) [35]. Their results, based on an expanded 2019–2020 dataset, show the same WSW–ENE maximum-compression direction and near-vertical minimum-stress axis as the present study.

The early post-seismic solution ($\phi \approx 0.546$, $\mu \approx 0.45$) in our analysis similarly indicates a more oblate stress configuration and a marked reduction in differential stress without rotation of the principal axes, capturing the short-term mechanical response of the crust immediately after the mainshock. This behavior is consistent with step-wise co-seismic stress-relaxation patterns documented in other compressional foreland settings [6], and with the iterative stress–fault orientation solutions of Vavryčuk (2014) [30], which show that early aftershock sequences often reflect transient weakening conditions rather than a permanent rotation of the stress tensor.

A compact numerical comparison of the stress orientations, ϕ and μ ratios, and their temporal evolution for the three inversion windows (regional, co-seismic, early post-seismic) is summarized in Table 2, providing a concise cross-window synthesis that highlights the stability of stress orientations and the transient reduction in stress anisotropy during the early sequence.

Table 2. Comparative stress parameters (azimuth/plunge in degrees).

Dataset / Stage	N	σ_1 (Az/Pl)	σ_3 (Az/Pl)	ϕ	μ
Tectonic-region: dr_planA	27	246.9 / 8.1	14.0 / 76.7	0.75	0.95
Tectonic-region: dr_planB	27	248.0 / 6.9	16.8 / 77.4	0.70	0.93
Co-seismic mainshock	1	245 / 32*	52 / 57*	—	—
Early post-seismic sequence	37†	239.5 / 12.5	57.2 / 77.5	0.546	0.45

* *Converted from plunge/azimuth in the TENSOR panel; $R = 0.23$. † N includes the mainshock*

4 Conclusions

The stress inversions for the regional, coseismic, and very-early post-seismic windows consistently define a compressional reverse-faulting regime along the Durrës–Tirana segment of the Adria–Albanides collision zone. The regional solutions indicate a stable WSW–ENE-directed σ_1 with shallow plunge (dr_planA: 246.9/8.1°, dr_planB: 248.0/6.9°) and a near-vertical σ_3 (dr_planA: 14.0/76.7°, dr_planB: 16.8/77.4°), accompanied by elevated ϕ and μ values (0.75/0.70; 0.95/0.93). The mainshock is fully compatible with this ambient configuration.

The early post-seismic stress tensor ($\sigma_1 = 239.5/12.5^\circ$, $\sigma_2 = 149.3/0.5^\circ$, $\sigma_3 = 57.2/77.5^\circ$) preserves the principal-stress orientations but shows reduced $\phi = 0.546$ and $\mu = 0.45$, reflecting a transient decrease in differential stress and a more oblate stress state immediately

after the mainshock. These changes represent short-lived coseismic relaxation without any rotation of the long-term regional stress field.

Overall, the Mw 6.4 Durrës earthquake sequence occurred within a persistent compressional regime, while the early aftershocks capture the immediate mechanical adjustment of the crust. This two-window comparison provides a robust and quantitative framework for characterizing stress evolution in compressional forelands of the Adria–Albanides system.

References

1. **Aliaj, S., Baldassarre, G., & Shkupi, D. (2000).** Seismotectonic map of Albania with an explanatory text. *Natural Hazards and Earth System Sciences*, *1*, 71–82.
2. **Aliaj, S., & Mesonjesi, A. (2022).** Periadriatic Foredeep (onshore Albania) Is Developed as a Dextral Pull-Apart Basin. *Bulletin of the Geological Society of Greece*, *59*(1), 118–157. <https://doi.org/10.12681/bgsg.31265>.
3. **Aliaj, S. (2020).** The November 26, 2019, Mw 6.4 Durrës earthquake and its relation to the geological structure of the Adria–Albanides collision margin. In *Proceedings of the International Symposium on Durrës Earthquakes and Eurocodes* (Tirana, Sept 21–22, 2020). https://fin.edu.al/wp-content/uploads/2024/04/ISDEE_Proceedings.pdf
4. **Papadopoulos, G. A., et al. (2020).** The Durrës, Albania, Mw 6.4 earthquake of 26 November 2019. *Seismological Research Letters*, *91*(6), 3171–3187. <https://doi.org/10.1785/0220200174>
5. **Meco, S., Aliaj, S., & Turku, I. (2000).** *Geology of Albania*. Gebrüder Borntraeger, Berlin–Stuttgart. ISBN 3-443-11028-2.
6. **Matraku, K., Jouanne, F., Dushi, E., Koçi, R., Kuka, N., Grandin, R., & Bascou, P. (2023).** The 26 November 2019 Durrës earthquake, Albania: Coseismic displacements and occurrence of slow slip events in the year following the earthquake. *Geophysical Journal International*, *234*(2), 807–826. <https://doi.org/10.1093/gji/ggad101>.
7. **Burchfiel, B. C., King, R. W., Todosov, A., Durmurdzanov, N., Serafimovski, T., & Nurce, B. (2006).** GPS results for Macedonia and its importance for the tectonics of the Southern Balkan extensional regime. *Tectonophysics*, *413*(3–4), 239–248. <https://doi.org/10.1016/j.tecto.2005.10.046>.
8. **D’Agostino, N., Avallone, A., Cheloni, D., D’Anastasio, E., Mantenuto, S., & Selvaggi, G. (2008).** Active tectonics of the Adriatic region from GPS and earthquake slip vectors. *Journal of Geophysical Research: Solid Earth*, *113*(B12), B12413. <https://doi.org/10.1029/2008JB005860>.
9. **Jouanne, F., Mugnier, J.-L., Koçi, R., Bushati, S., Matev, K., Kuka, N., Shinko, I., & Kabo, M. (2012).** GPS constraints on current tectonics of Albania. *Tectonophysics*, *554–555*, 50–62. <https://doi.org/10.1016/j.tecto.2012.06.008>
10. **Muço, B. (1994).** Focal mechanism solutions for Albanian earthquakes for the years 1964–1988. *Tectonophysics*, *231*(4), 311–323. [https://doi.org/10.1016/0040-1951\(94\)90041-8](https://doi.org/10.1016/0040-1951(94)90041-8).
11. **Muço, B. (2007).** Focal mechanism solutions and stress field distribution in Albania. *Albanian Journal of Natural & Technical Sciences*, *1*, 129–134.
12. **Kiratzis, A., & Dimakis, E. (2013).** Focal mechanisms and slip models of moderate-size earthquakes in Albania and adjacent countries. *Italian Journal of Geosciences*, *132*(2), 186–193. <https://doi.org/10.3301/IJG.2011.33>.

13. **Baker, C., Hatzfeld, D., Lyon-Caen, H., Papadimitriou, E., Rigo, A., & Deschamps, A. (1997).** Earthquake mechanisms of the Adriatic Sea and western Greece. *Geophysical Journal International*, *131*(3), 559–594.
14. **Ormeni, R., Hoxha, I., Gjuzi, O., Bozo, Rr., Gega, D., Kanani, Xh., Mucaj, D., Piccardi, L., Vittori, E., Blumetti, A. M., Di Manna, P., & Comerci, V. (2022).** The catalogue of earthquakes focal mechanisms occurred in Albania and its surrounding during 1948 to 2022. *EAGE/EarthDoc*. <https://doi.org/10.3997/2214-4609.202220159>.
15. **Konstantinou, K. I., Melis, N. S., & Boukouras, K. (2010).** Routine regional moment tensor inversion for earthquakes in the Greek region: The NOA database (2001–2006). *Seismological Research Letters*, *81*(5), 750–760. <https://doi.org/10.1785/gssrl.81.5.750>.
16. **Papazachos, B., Kiratzi, A., & Papazachos, C. (2000).** Rates of active crustal deformation and recurrence of large earthquakes in the Aegean and surrounding area. *Tectonophysics*, *319*(1), 285–303. [https://doi.org/10.1016/S0040-1951\(00\)00048-8](https://doi.org/10.1016/S0040-1951(00)00048-8).
17. **Roumelioti, Z., Kiratzi, A., & Benetatos, C. (2011).** Time-domain moment tensors for shallow earthquakes in the broader Aegean Sea: 2006–2007 AUTC database. *Journal of Geodynamics*, *51*, 179–189. <https://doi.org/10.1016/j.jog.2010.07.001>.
18. **Moshou, A., & Dushi, E. (2019).** A preliminary report on the 26 November 2019 Mw = 6.4 Durrës, Albania earthquake. *European-Mediterranean Seismological Centre*, Essonne, France, 12 pp.
19. **PyGMT Developers (2025).** PyGMT: A Python interface for the Generic Mapping Tools (v0.16.0). *Zenodo*. <https://doi.org/10.5281/zenodo.3781524>.
20. **Wessel, P., Luis, J. F., Uieda, L., Scharroo, R., Wobbe, F., Smith, W. H. F., & Tian, D. (2019).** The Generic Mapping Tools Version 6. *Geochemistry, Geophysics, Geosystems*, *20*(11), 5556–5564. <https://doi.org/10.1029/2019GC008515>.
21. **Sokos, E. N., & Zahradnik, J. (2008).** ISOLA: A Fortran code and a Matlab GUI to perform multiple-point source inversion of seismic data. *Computers & Geosciences*, *34*(8), 967–977. <https://doi.org/10.1016/j.cageo.2007.07.005>.
22. **Dushi, E., Minarolli, A., Kasaj, E., & Gjuzi, O. (2014).** Focal mechanism solutions for local earthquakes ($M > 3.0$) from Albanian Seismological Network broadband recordings. In: *XX Congress of the Carpathian–Balkan Geological Association (CBGA)*, Tirana, Vol. I, Session G05.
23. **Dushi, E., Koçi, R., Begu, E., & Bozo, Rr. (2018).** Stress inversion from the focal mechanism of moderate earthquakes in Albania. *SGEM 2018*, *18*(1.1), 989–996. <https://doi.org/10.5593/sgem2018/1.1/S05.123>.
24. **Delvaux, D., & Sperner, B. (2003).** New aspects of tectonic stress inversion with reference to the TENSOR program. In: Nieuwland, D. A. (Ed.), *New Insights into Structural Interpretation and Modelling*. Geological Society, London, Special Publications 212, 75–100. <https://doi.org/10.1144/GSL.SP.2003.212.01.06>.
25. **Bott, M. H. P. (1959).** The mechanics of oblique slip faulting. *Geological Magazine*, *96*(2), 109–117.
26. **Wallace, R. E. (1951).** Geometry of shearing stress and relation to faulting. *Geological Society of America Bulletin*, *62*(12), 1317–1340.
27. **Michael, A. J. (1984).** Determination of stress from slip data: Faults and focal mechanisms. *Journal of Geophysical Research: Solid Earth*, *89*(B13), 11517–11526. <https://doi.org/10.1029/JB089iB13p11517>.
28. **Michael, A. J. (1987).** Use of focal mechanisms to determine stress: A control study. *Journal of Geophysical Research: Solid Earth*, *92*(B1), 357–368. <https://doi.org/10.1029/JB092iB01p00357>.

29. **Wiemer, S. (2001)**. A software package to analyze seismicity: ZMAP. *Seismological Research Letters*, 72(3), 373–382. <https://doi.org/10.1785/gssrl.72.3.373>
30. **Vavryčuk, V. (2014)**. Iterative joint inversion for stress and fault orientations from focal mechanisms. *Geophysical Journal International*, 199(1), 69–77. <https://doi.org/10.1093/gji/ggu224>
31. **Govorčin, M., Wdowinski, S., Matoš, B., & Funning, G. J. (2020)**. Geodetic source modeling of the 2019 Mw 6.3 Durrës, Albania, earthquake: Partial rupture of a blind reverse fault. *Geophysical Research Letters*, 47, e2020GL088990. <https://doi.org/10.1029/2020GL088990>
32. **Ahern, T., Casey, R., Barnes, D., & Trabant, C. (2019)**. The International Federation of Digital Seismograph Networks (FDSN): An integrated system of seismological data services. *Seismological Research Letters*, 90(3), 1098–1104. <https://doi.org/10.1785/0220180251>.
33. **Dieterich, J. H. (1979)**. Modeling of rock friction: 1. Experimental results and constitutive equations. *Journal of Geophysical Research*, 84, 2161–2168. <https://doi.org/10.1029/JB084iB05p02161>
34. **Teloni, S., Invernizzi C., Mazzoli S., Pierantoni P. P., Spina V. (2021)**. Seismogenic fault system of the Mw 6.4 November 2019 Albania earthquake. *Journal of the Geological Society*, 178(2). <https://doi.org/10.1144/jgs2020-193>
35. **Heidbach, O., Rajabi, M., Reiter, K., & Ziegler, M. (2016)**. World Stress Map database release 2016. GFZ Data Services. <https://doi.org/10.5880/WSM.2016.001>